SUPPORTING INFORMATION FOR THE MANUSCRIPT

ENSO and NAO affect long-term leaf litter dynamics and stoichiometry of Scots pine and European beech mixedwoods

https://doi.org/10.1111/gcb.14672

Ester González de Andrés[1], Juan A. Blanco[1,*], J. Bosco Imbert[1], Biing T. Guan[2], Yueh-Hsin Lo[1], Federico J. Castillo[1]

[1] Departamento de Ciencias, Universidad Pública de Navarra, Campus de Arrosadía, Pamplona, Navarra, 31006, Spain.

[2] School of Forestry and Resource Conservation, National Taiwan University, Taipei, 10617, Taiwan, Republic of China

Running head: Links between global climate and tree litter

Correspondence:

Juan A. Blanco, Departamento de Ciencias, Universidad Pública de Navarra, Campus de Arrosadía, Pamplona, Navarra, 31006, Spain.

E-mail: juan.blanco@unavarra.es

Phone: (+34) 948 16 9859

Key words: leaf litter, nutrient cycling, ensemble empirical mode decomposition (EEMD), *Fagus sylvatica*, nutrient limitation, *Pinus sylvestris*, Pyrenees, stoichiometry, structural equation model (SEM).

APPENDIX A. Study area and climatic data

The study area is located in the Spanish Pyrenees (province of Navarre) close to the southwestern distribution limit of both species (Fig. S1). The research forests are even-aged Scots pine stands resulting from successful natural regeneration after clear-cuttings carried out in the early and mid-1960s. Over recent decades, European beech growth under pine canopy has progressively resulted in mixed stands, particularly at the Mediterranean site.

In order to evaluate the impact of climatic conditions on leaf litter dynamics, radial growth, and water-use series, daily historical climate data (maximum and minimum temperature and precipitation) for the period 2000-2017 were obtained from the nearest weather stations to each site. Due to the large elevation difference between the continental site and the closest weather station (over 600 m), the mountain microclimate simulation model MT-CLIM (Running et al., 1987) was applied to correct climate data (Lo et al., 2011). Maximum and minimum temperature lapse rates and precipitation isohyets needed for extrapolation were calculated from regional climate data. Missing data were calculated by interpolating values from nearby weather stations.

Monthly local climate data were transformed into a more biologically meaningful variable that informs about soil water condition: the standardized precipitation evaporation index (SPEI). The SPEI.*X* is a multi-scalar index, where *X* refers to the time scale in months at which it is calculated. This index includes both precipitation and temperature influence in droughts by means of the evapotranspiration processes (Vicente-Serrano et al., 2010). It has shown an improved capability to identify drought impacts when compared with other commonly used drought indices (e.g. Vicente-Serrano et al., 2012). The SPEI is based on a monthly climatic water balance (precipitation minus potential evapotranspiration, PET), which is adjusted using a three-parameter log–logistic distribution. PET was estimated following Thornthwaite & Mather (1957) and the *SPEI* package (Beguería & Vicente-Serrano, 2017) from R software was used to calculate SPEI at time scales of 1 and 3 months.

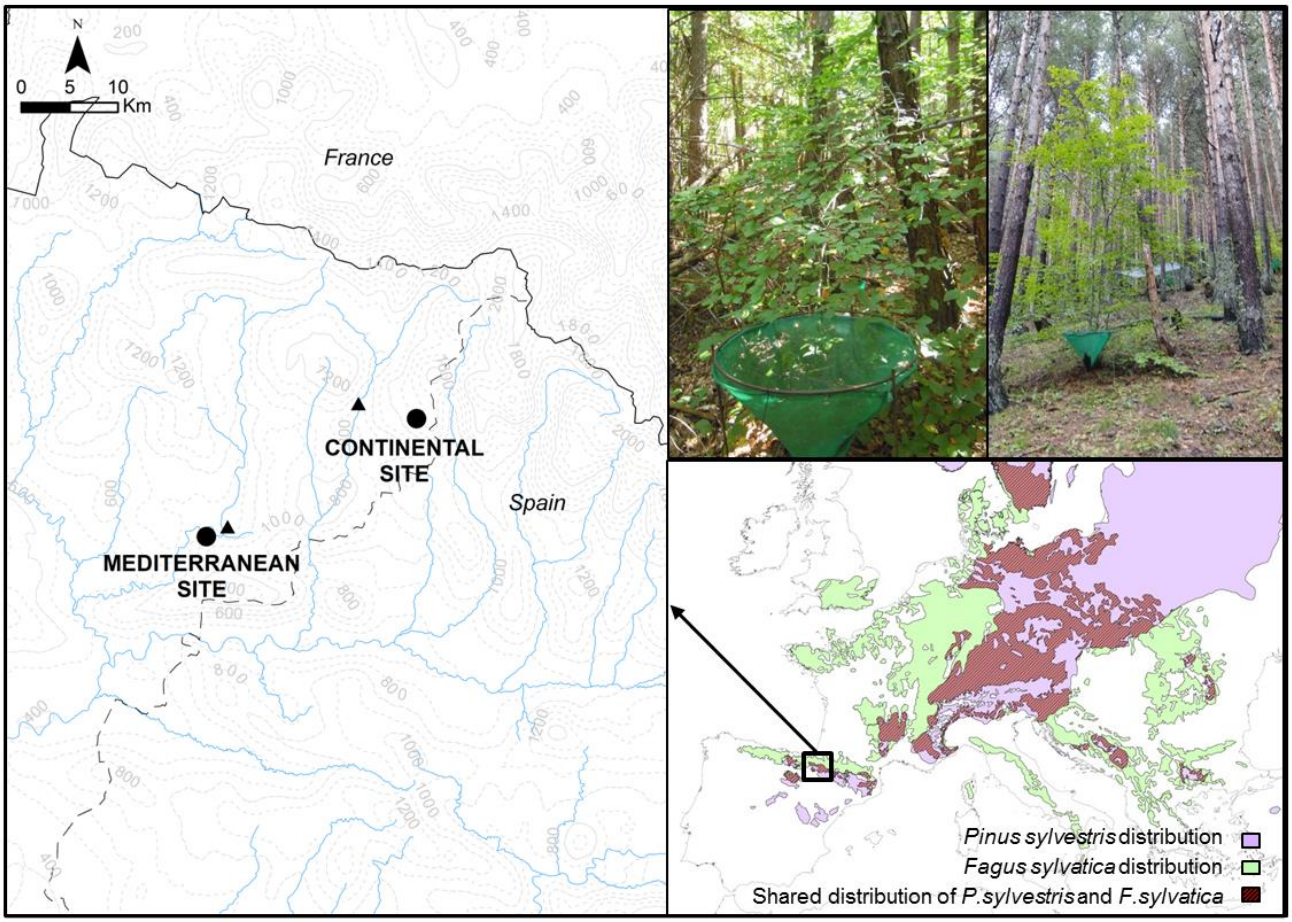

Figure S1. Location of experimental plots (circles) and weather stations providing climatic date (triangles). The map in the lower right shows the natural European distribution of Scots pine (*Pinus sylvestris* L.) and European beech (*Fagus sylvatica* L.) (modified from EUFORGEN, 2009a; EUFORGEN, 2009b) and the overlap area between both species. Upper right pictures show images of litter traps in the Mediterranean stand (left) and in the continental stand (right).

APPENDIX B. Trendless components

Time series of climate and leaf litter biomass and nutrient composition were decomposed using the ensemble empirical mode decomposition (EEMD) methodology into trendless components (TCs) (Fig. S2, S3 and S4) and a residual or trend.

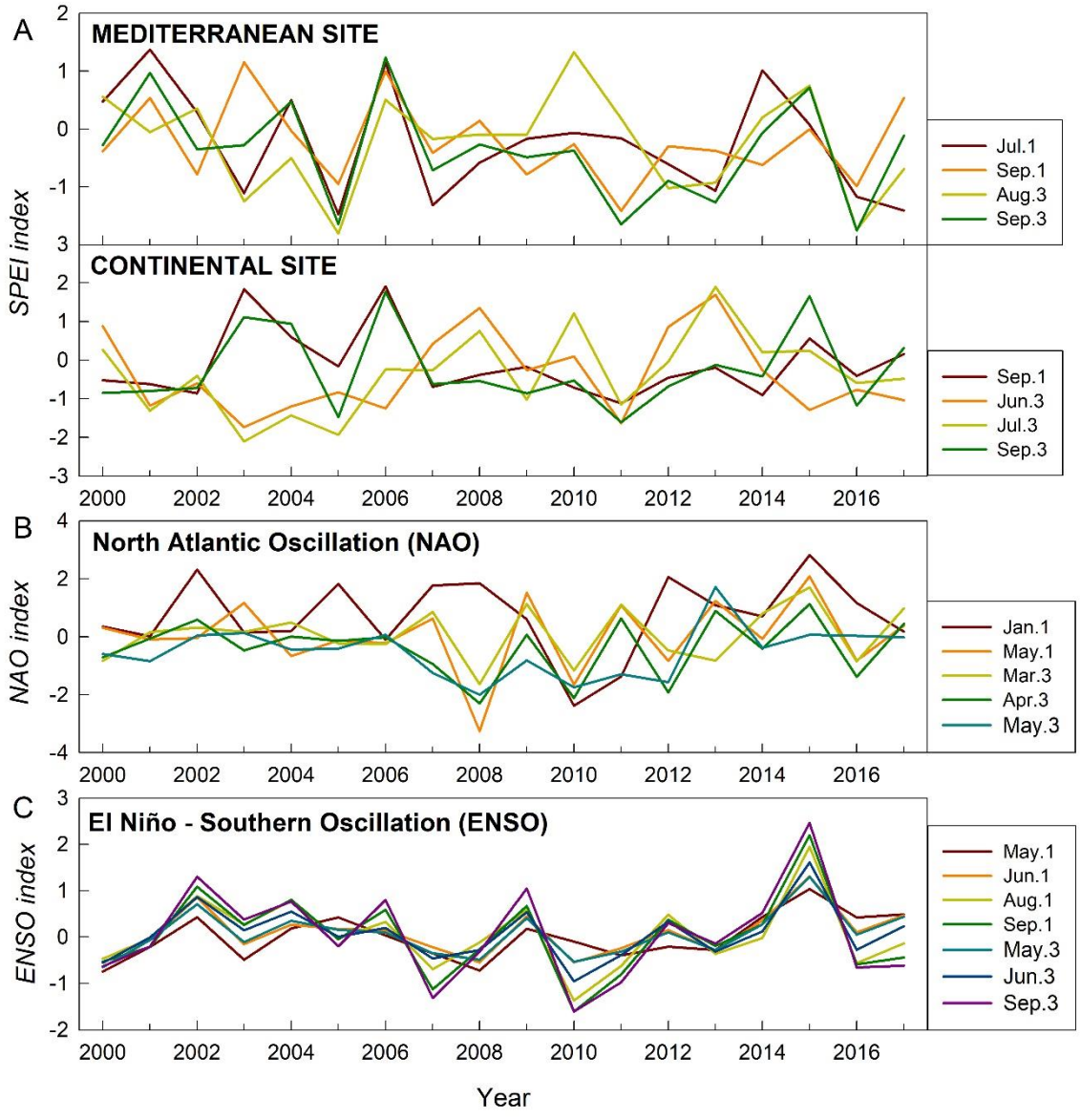

Figure S2. Trendless components (TCs) of standardized precipitation evaporation index (SPEI) at the study sites (A), North Atlantic Oscillation (NAO) (B), and El Niño – Southern Oscillation (ENSO) (C) during the period of litter traps' experiment. Variables included in further analysis are shown. Variables are presented as *Month.X*, where *Month* in the last month considered for index calculation and *X* is the time scale in months. TCs were extracted by means of ensemble empirical mode decomposition (EEMD) as the sum of the intrinsic mode functions (IMFs).

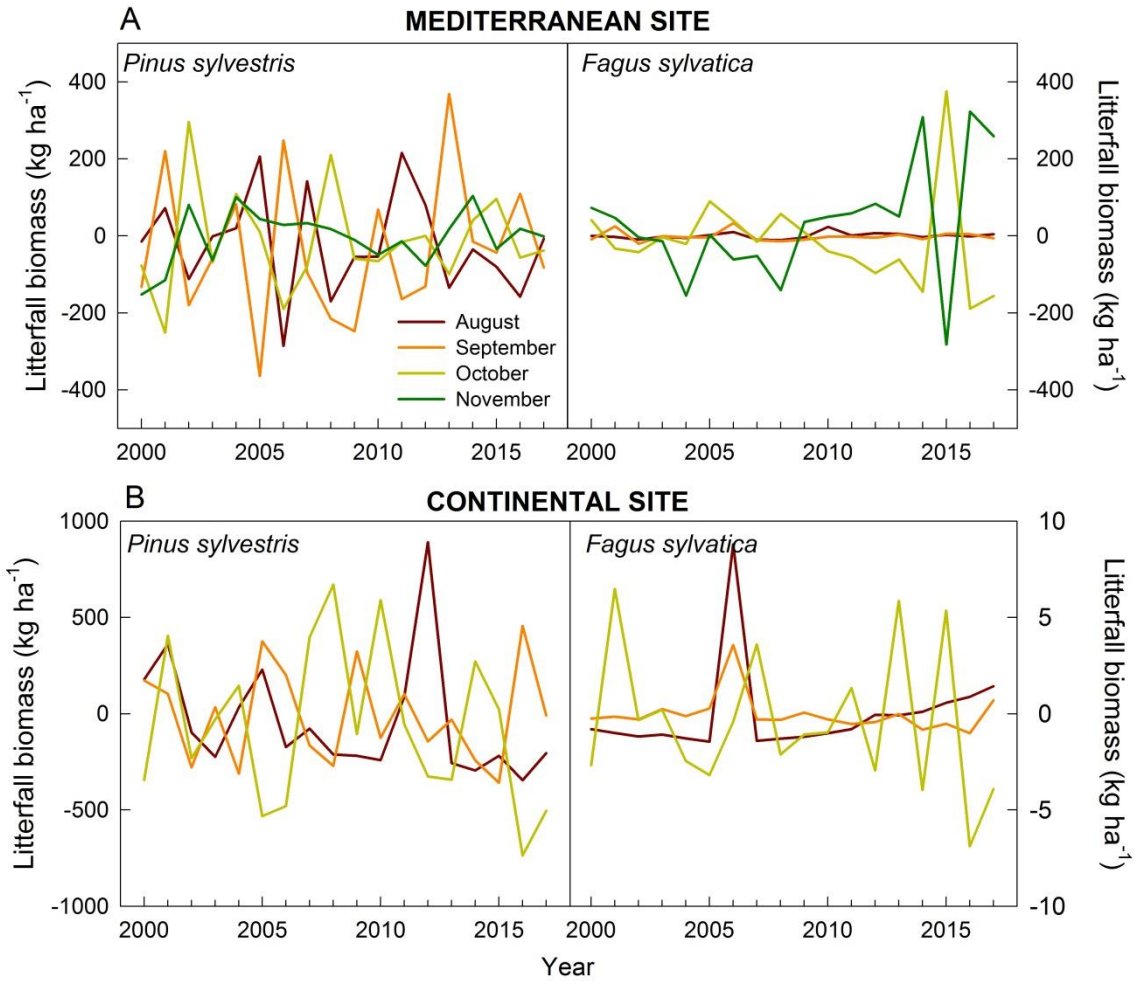

Figure S3. Trendless components (TCs) of monthly leaf litter production of Scots pine (*Pinus sylvestris*, left) and European beech (*Fagus sylvatica*, right) at the Mediterranean site (A) and continental site (B). TCs were extracted by means of ensemble empirical mode decomposition (EEMD) as the sum of the intrinsic mode functions (IMFs). Different colors represent different month.

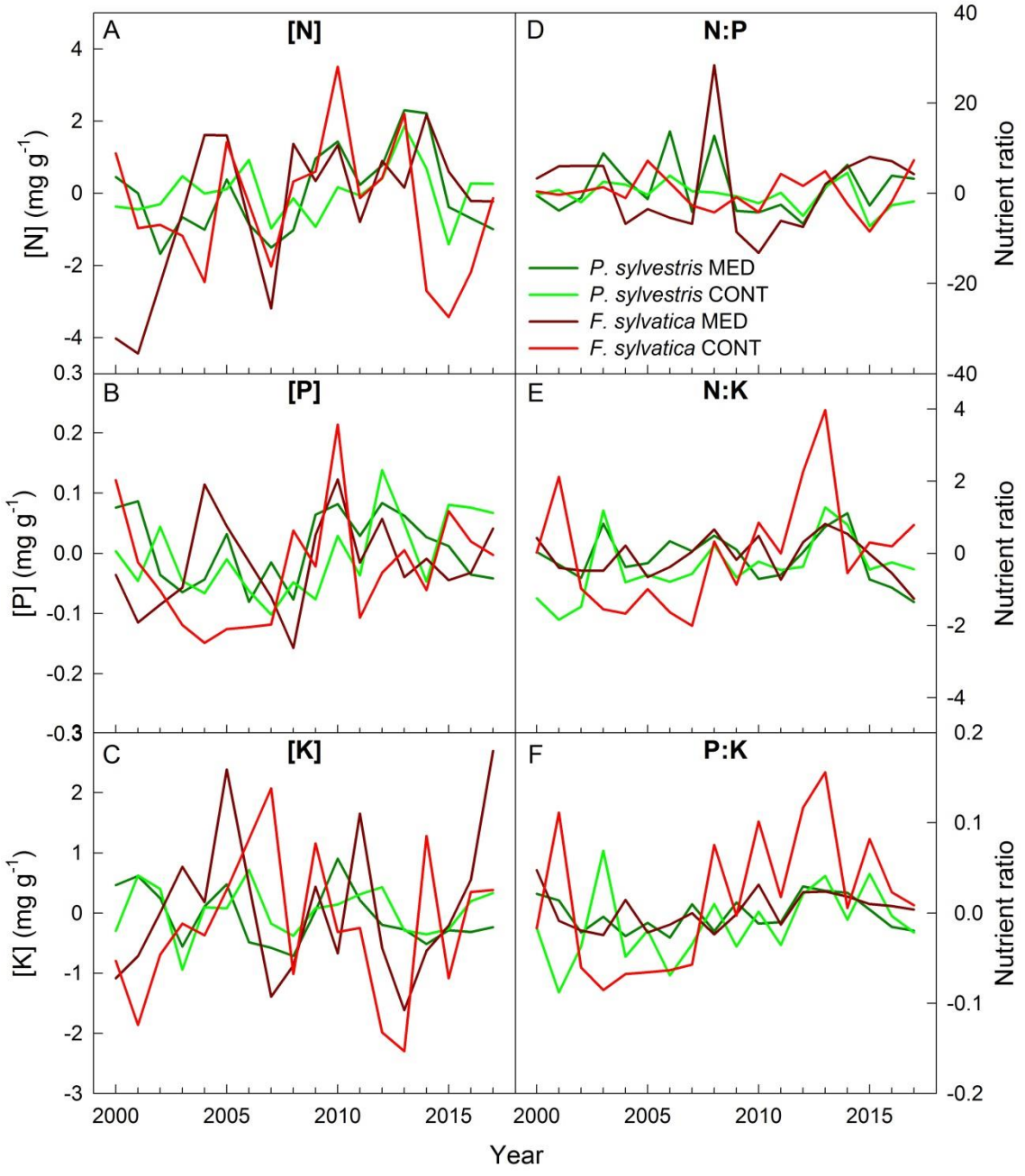

Figure S4. Trendless components (TCs) of concentration of nitrogen ([N]), phosphorous ([P]) and potassium ([K]) and stoichiometric ratios N:P, N:K and P:K of litterfall of Scots pine (*Pinus sylvestris*, green) and European beech (*Fagus sylvatica*, red) collected at the two study sites: Mediterranean site (dark) and continental site (light). TCs were extracted by means of ensemble empirical mode decomposition (EEMD) as the sum of the intrinsic mode functions (IMFs).

Despite TCs were calculated as the sum of a small number of oscillatory components (intrinsic mode functions, IMFs), in general they did not exhibit a marked oscillatory behavior (Table S1).

Table S1. Partial autocorrelation function (pacf) of trendless components (TCs) of leaf litter series of biomass and nutrient composition of Scots pine (*Pinus sylvestris*) and European beech (*Fagus sylvatica*) at the two study sites for time lags up to 18 years. Lag at which pacf is significant is shown in brackets.

	Pinus sylvestris		*Fagus sylvatica*	
	MED site	CONT site	MED site	CONT site
$Litter_{annual}$	n.s.	n.s.	n.s.	n.s.
$Litter_{Aug}$	n.s.	n.s.	n.s.	n.s.
$Litter_{Sep}$	n.s.	n.s.	-0.463 (lag = 4)	n.s.
$Litter_{Oct}$	-0.459 (lag = 5)	n.s.	n.s.	n.s.
$Litter_{Nov}$	n.s.	-	n.s.	-
[N]	0.488 (lag = 1)	n.s.	n.s.	-0.491 (lag = 6)
[P]	n.s.	n.s.	n.s.	n.s.
[K]	-0.473 (lag = 2)	n.s.	n.s.	-0.547 (lag = 6)
N:P	n.s.	n.s.	n.s.	n.s.
N:K	n.s.	n.s.	n.s.	n.s.
P:K	n.s.	n.s.	n.s.	n.s.

APPENDIX C. Teleconnections of local climate

Significant correlations between atmospheric-oceanic oscillation indices and the trendless components (TCs) of local climate variables were found for the period 2000 - 2017. Precipitation displayed contrasting correlations with large-scale indices: negative with NAO and positive with ENSO. In the former case, previous winter NAO negatively impacted June precipitation at the Mediterranean site (r = -0.806, $p < 0.001$), and May and June precipitation at the continental site (r = -0.760, $p < 0.001$). Besides, previous September NAO had a negative correlation with February precipitation (MED site: r = -0.703, p = 0.002; CONT site: r = -0.697, p = 0.001). Therefore, NAO impacts on western Pyrenean precipitation had a delay on several months. On the other hand, $ENSO_{July}$ exerted a positive influence on August precipitation (MED site: r = 0.672, p = 0.002; CONT site: r = 0.600, p = 0.008). $NAO_{February\text{-}March}$ exerted the greatest influence on mean temperature from the same period (MED site: r = 0.641, p = 0.004; CONT site: r = 0.645, p = 0.003). Mean October to December temperature showed positive correlations with $ENSO_{October\text{-}December}$ at the Mediterranean site (r = 0.656, p = 0.003) and mean November and December temperature was positive correlated with $ENSO_{November\text{-}December}$ at the continental site (r = 0.484, p = 0.042).

Spatiotemporal correlations of local climate and gridded fields for the period 2000 – 2017 were consistent with those found for large-scale circulation indices. On one hand, summer precipitation was negatively correlated with previous winter North Atlantic Ocean SLP (NAO influence area) (Fig. S5A) and summer precipitation positively responded to summer tropical

Pacific Ocean SST (ENSO influence area) (Fig. S5B). On the other hand, late winter and early spring mean temperatures were positively associated with SLP in the North Atlantic during the same period (Fig. S5C). Autumn mean temperature was positively related with autumn Pacific Ocean SST (Fig. S5D).

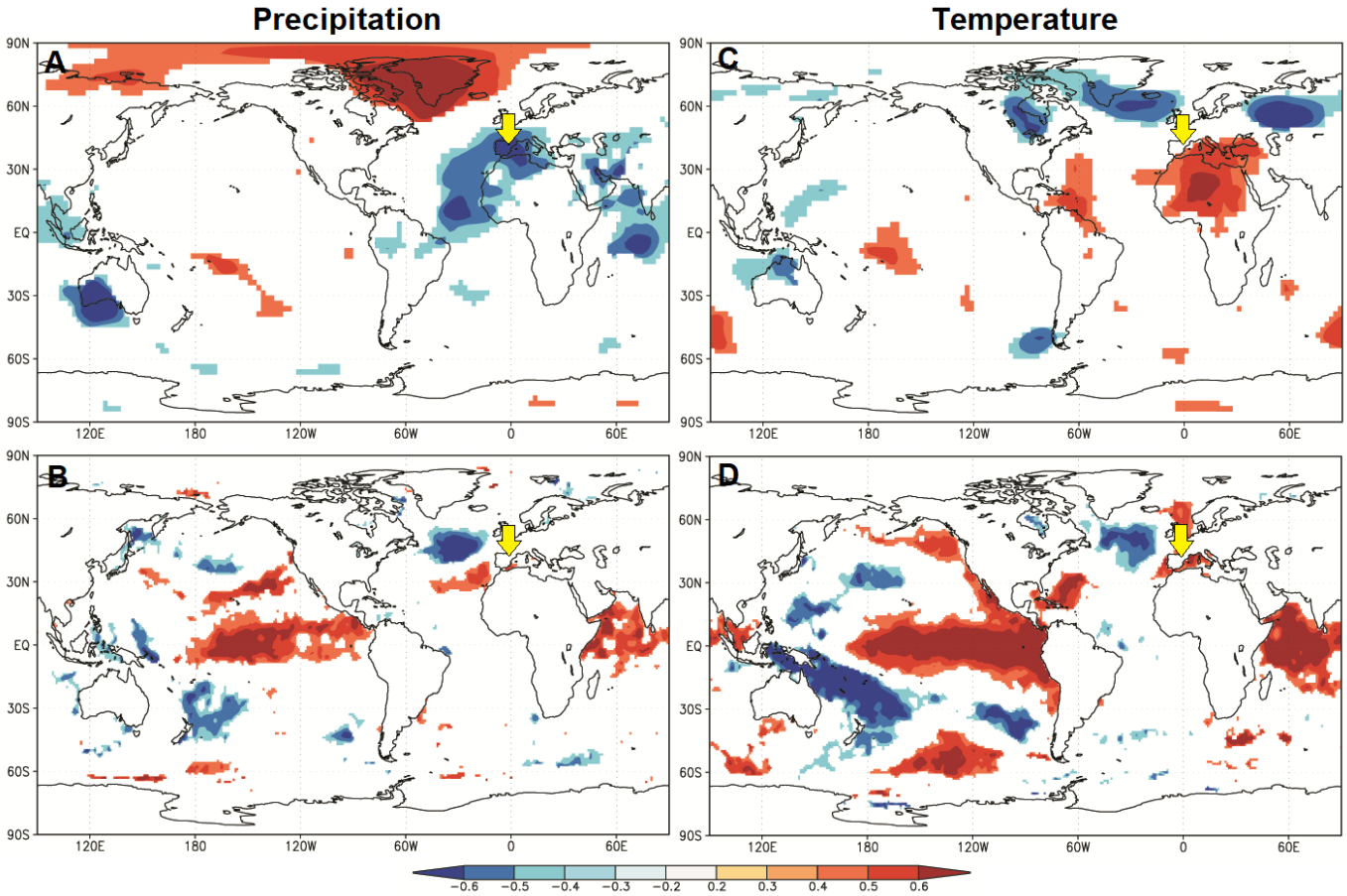

Figure S5. Spatiotemporal correlations between detrended NCEP/NCAR R1 sea level pressure (SLP, above) and detrended HadISST1 sea surface temperature (SST; bottom) and trendless components (TCs) of local climate datasets for the time period 2000 – 2017: (A) previous December SLP – June and July precipitation; (B) July to August SST – August precipitation; (C) February SLP – February to March mean temperature; (D) October to December SST – October to December mean temperature. Correlations with $p < 0.1$ are shown. Because of high similarities with the continental site correlation patterns, only correlations of local climate from the Mediterranean site are presented. Yellow arrows indicate location of the study sites.

Our results show that natural SLP variability in the North Atlantic Ocean is significantly correlated with local climate variables from the western Pyrenees (Figs. S5A and S5C). The NAO is the most important source of climate variability in Europe in general (Hurrel, 1995; Trigo et al., 2002), and in the Iberian Peninsula in particular (Trigo et al., 2004; Gómez-Navarro

et al., 2011). Consistently, we found a significant effect on February and March temperature (Fig. S5C), which is also in accord with the findings of Castro-Díez et al. (2002). NAO appears to be one of the main climatic mechanisms influencing rainfall variability in the Southern Pyrenees (Morellón et al., 2012). Although weak relationships are generally reported for NAO and summer rainfall (Gallego et al., 2005), our results showed the strongest correlation between winter NAO and late spring and early summer precipitation (Fig. S5A). However, regional advection of heat and humidity transport associated with a given phase of NAO may propagate until summer months (May-September) due to the memory effects of snow cover (Barriopedro et al., 2006) and soil moisture (Quesada et al., 2012).

In addition, climate and hydrological conditions in the Pyrenees are transitional between Atlantic and Mediterranean influences, being therefore not only affected by NAO but also by other atmospheric dynamics operating at larger distances such as ENSO (Rodó et al., 1997; Pozo-Vazquez et al., 2005; Gámiz-Fortis et al., 2011). ENSO represents the strongest inter-annual variation of Earth's climate affecting a wide range of geographic areas (Stenseth et al., 2003). We found significant relationships between ENSO and Pyrenean climate (Figs. S5B and S5D). Despite the Iberian Peninsula is not located in the main area of influence of ENSO (Mason & Goddard, 2001), several studies have reported extratropical responses to tropical SST anomalies (e.g. Mariotti et al., 2002; Pozo-Vázquez et al., 2005; Brönnimann et al., 2007; Shaman & Tziperman, 2011; Losada et al., 2012). Particularly, negative SLP events are expected in Northern Spain during positive phases of ENSO (Pozo-Vázquez et al. 2005; Brönnimann et al., 2007), which translates into increased summer rainfall following the above explanation just as our results showed. Such link between ENSO and Mediterranean climate seems to have increased at the end of the 20th century (Mariotti et al., 2002).

APPENDIX D. List of collaborators

The time series of litterfall production used in this analysis are a collective effort of many students, postdoctoral fellows, professors, and volunteers of the Ecology and Environmental Group working at the School of Agricultural Engineering of the Public University of Navarre (Pamplona, Spain). Without their time and effort, sustaining for 19 years the sampling collection, preparation and analysis would have been impossible. The authors want to acknowledge the work of all of them, for which we are very thankful (Table S2).

Table S2. List of people involved in the collection and generation of the litterfall data series in the period 2000-2018.

Name		
Alberto Alfonso	Carlos E. Blanco	María Resano
Mikel Agós	David Candel-Pérez	Roberto Rípodas
Maria Ansó	Yenny Castrillón	Miguel Salvador
Maria Arias	María Durán	Iván Sánchez
Arkaitz Arretxe	Cristina Eslava	Leticia San Emeterio
Jon Aspurz	Ximena Herrera	Amaia Sesma
Iñigo Auzmendi	Iñigo Iriarte	Iker Tres
Andrea Azpiroz	Diego Luqui	Maitane Unzu
Ion Beraza	Carmen Martínez	Jennifer Yeoung
Asier Bermejo	Ieltxu Oteiza	Antonio Yeste
Roberto Blanco	Beatriz Pérez	Itziar Zabala
	Irantzu Primicia	Xabier Zendegui

REFERENCES

Barriopedro D., García-Herrera R., Hernández, E. (2006) The role of snow cover in the Northern Hemisphere winter to summer transition. *Geophysical Research Letters*, **33**, L14708.

Beguería S., Vicente-Serrano S.M. (2017) SPEI: Calculation of the Standardised Precipitation-Evapotranspiration Index. R package version 1.7. https://CRAN.R-project.org/package=SPEI

Brönnimann S., Xoplaki E., Casty C., Pauling A., Luterbacher J. (2007) ENSO influence on Europe during the last centuries. *Climate Dynamics*, **28**, 181–197.

Castro-Díez Y., Pozo-Vázquez D., Rodrigo F.S., Esteban-Parra M.J. (2002) NAO and winter temperature variability in southern Europe. *Geophysical Research Letters*, **29**, 1160.

EUFORGEN (2009a) Distribution map of Beech (*Fagus sylvatica*). http://www.euforgen.org.

EUFORGEN (2009b) Distribution map of Scots pine (*Pinus sylvestris*), http://www.euforgen.org.

Gallego M.C., García J.A., Vaquero J.M. (2005) The NAO signal in a daily rainfall series over the Iberian Peninsula. *Climate Research*, **29**, 103-109.

Gámiz-Fortis S.R., Hidalgo-Muñoz J.M., Argüeso D., Esteban-Parra M.J., Castro-Díez Y. (2011) Spatio-temporal variability in Ebro river basin (NE Spain): Global SST as potential source of predictability on decadal time scales. *Journal of Hydrology*, **409**, 759-775.

Gómez-Navarro J.J., Montávez J.P., Jerez S., Jiménez-Guerrero P., Lorente-Plazas R., González-Rouco J.F., Zorita E. (2001) A regional climate simulation over the Iberian Peninsula for the last millennium. *Climate of the Past*, **7**, 451–472.

Hurrell J.W. (1995) Decadal trends in the North Atlantic Oscillation: regional temperatures and precipitation. *Science*, **269**, 676–679.

Lo Y.H., Blanco J.A., Seely B., Welham C., Kimmins J. P. (2011) Generating reliable meteorological data in mountainous areas with scarce presence of weather records: The performance of MTCLIM in interior British Columbia, Canada. *Environmental Modelling & Software*, **26**, 644–657.

Losada T., Rodríguez-Fonseca B., Kucharski F. (2012) Tropical influence on the summer Mediterranean climate. *Atmospheric Science Letters*, **13**, 36–42.

Mariotti A, Zeng N, Lau K-M. (2002) Euro-Mediterranean rainfall and ENSO-A seasonally varying relationship. *Geophysical Research Letters*, **29**, 1621.

Mason S.J., Goddard L. (2001) Probabilistic precipitation anomalies associated with ENSO. *Bulletin of the American Meteorological Society*, **82**, 619-638.

Morellón M., Pérez-Sanz A., Corella J.P., Büntgen U. *et al.* (2012) A multi-proxy perspective on millenium-long climate variability in the Southern Pyrenees. *Climate of the Past*, **8**, 683-700.

Pozo-Vázquez D., Gámiz-Fortis S.R., Tovar-Pescador J., Esteban-Parra M.J., Castro-Díez Y. (2005) El Niño–Southern Oscillation events and associated European winter precipitation anomalies. *International Journal of Climatology*, **25**, 17–31.

Quesada B., Vautard R., Yiou P., Hirschi M., Seneviratne, S.I. (2012) Asymmetric European summer heat predictability from wet and dry southern winters and springs. *Nature Climate Change*, **2**, 736–741.

Rodó X., Baert E., Comin F. (1997) Variations in seasonal rainfall in Southern Europe during the present century: relationships with the North Atlantic Oscillation and the El Niño-Southern Oscillation. *Climate Dynamics*, **13**, 275–284.

Running S.W., Nemani R.R., Hungerford R.D. (1987) Extrapolation of synoptic meteorological data in mountainous terrain and its use for simulating forest evapotranspiration and photosynthesis. *Canadian Journal of Forest Research*, **17**, 472–483.

Shaman J., Tziperman E. (2011) An atmospheric teleconnection linking ENSO and southwestern European precipitation. *Journal of Climate* **24**, 124-139.

Stenseth N.C.,Ottersen G., Hurrell J.W., Mysterud A., Lima M., Chan K.S., Yoccoz N.G., Ådlandsvik B. (2003) Studying climate effects on ecology through the use of climate indices: the North Atlantic Oscillation, El Niño-Southern Oscillation and beyond. *Proceedings of the Royal Society London B*, **270**, 2087–2096.

Trigo R.M., Osborn T.J., Corte-Real, J.M. (2002) The North Atlantic Oscillation influence on Europe: climate impacts and associated physical mechanisms. *Climate Research*, **20**, 9–17.

Trigo R.M., Pozo-Vazquez D., Osborn T.J., Castro-Díez Y., Gamiz-Fortis S., Esteban-Parra, M.J. (2004). North Atlantic oscillation influence on precipitation, river flow and water resources in the Iberian Peninsula. *International Journal of Climatology*, **24**, 925–944 .

Vicente-Serrano S.M., Beguería S., López-Moreno J.I. (2010) A multiscalar drought index sensitive to global warming: the standardized precipitation evapotranspiration index. *Journal of Climate*, **23,** 1696-1718.

Vicente-Serrano S.M., Beguería S., Lorenzo-Lacruz J., Camarero J.J., López-Moreno J.I., Azorin-Molina C., Revuelto J., Morán-Tejeda E., Sanchez-Lorenzo A. (2012) Performance of drought indices for ecological, agricultural, and hydrological applications. *Earth Interactions*, **16**, 1-27.